

DEM MODELLING

In previous work [8], a Grease Discrete Element Model (GDEM) was developed as recalled in Fig. 1(a). A discontinuous vision of the grease is proposed through the interaction of a set of elementary volumes. Thus, grease is represented as a collection of two kinds of particles: oil particles, that represents the viscous fluid and PTFE particles that represents the thickener.

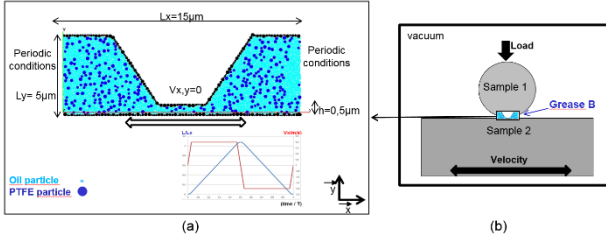


Figure 1. (a) GDEM model developed with its inputs [Busquet2017], (b) experimental set-up in previous work [9]

The resulting model is subjected to tribological-like conditions close to those applied in previous experimental work [9]; ie confinement and shearing between two bodies (cf. Fig. 1(b)). This grease discretization involves the definition of five interactions, each associated to a couple of parameters, as synthesized in Table 1: three “volume” interactions (oil/oil, PTFE/PTFE and oil/PTFE) and two “surface” interactions (oil/boundary and PTFE/boundary). For example, the oil/PTFE interaction should account for the chemical affinities between PTFE particles and oil while the oil/oil interaction should ensure that the whole set of oil particles matches on an average sense to the oil behavior at the macroscopic scale.

Interaction	Volume			Surface	
	oil / oil	PTFE / PTFE	oil / PTFE	oil / boundary	PTFE / boundary
Schematics					
Parameters involved (γ : force, dw : distance between 2 particles)	γ_{oo}, dw_{oo}	γ_{pp}, dw_{pp}	γ_{op}, dw_{op}	γ_{ob}, dw_{ob}	γ_{pb}, dw_{pb}

Table 1. Definition of the five interactions involved in the biphasic discrete element model

The identification procedure of the interaction parameters was based on rheometer-like simulations. Indeed, the relevant parameters for reproducing the macroscopic behavior of the B-type grease considered in terms of viscosity were determined. Several parameter combinations were shown to be possible for a given macroscopic behavior. However, the order of magnitude of the sets of parameters determined can be used as starting points for the tribological model.

As no measure was available for the couples of

parameters (γ, dw), a parametric study was performed on the GDEM subjected to tribological conditions and a selection of results are presented here. In Fig. 2, the grease structural changes is respectively plotted for low (Fig. 2(a1)) and high (Fig. 2(a2)) adhesion between PTFE and boundary. Simulation results are presented for a B-type granulometry and a selected “volume” combination, among the different solutions available (Strong relative interaction between oil/PTFE with respect to PTFE/PTFE In view to investigate the evolution of particle distribution and the friction factor, a cyclic motion is given to the lower boundary in the X-direction (Fig. 1(a)). Lateral periodic conditions are imposed to model an infinite contact and maintain a grease reserve. At the end of each simulation, an image is extracted to visualise the grease behavior.

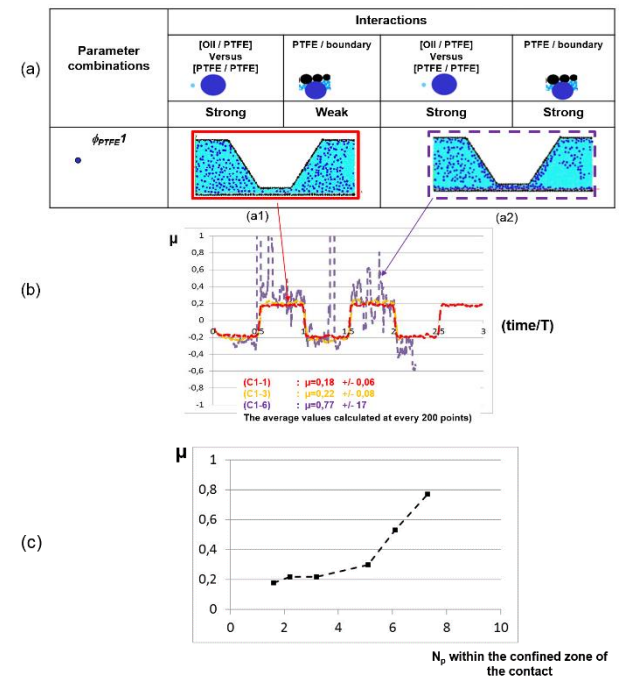


Figure 2. (a) Different tribological tendencies, (b) Evolution of the friction factor μ for the considered combinations, (c) evolution of the friction factor μ versus (N_p), the number of particles within the confined zone of the contact.

For strong relative influence of the (oil/PTFE) interaction with respect to the (PTFE/PTFE) interaction and weak PTFE/boundary ones, the behavior is homogeneous (cf. Fig. 2(a1)); the initial distribution of the PTFE particles remains unchanged. The PTFE particles “follow” the oil flow entrained by the driving boundary surface within the confined zone of the convergent, where only a few particles can be observed. For stronger adhesion (Fig. 2(a2)), it can be observed that the moving boundary surface attracts and entrains the PTFE particles within the confined zone, forming a “solid-like” layer with a high PTFE particle concentration. Under such conditions, the

number of PTFE particles within the confined zone of the contact and the number of particles “stuck” on the moving surface seems to increase. In terms of resulting friction, in Fig. 2(b), the friction factor (denoted μ) is plotted versus time for the two considered combinations. The average value of μ seems to increase with adhesion (so does the friction standard deviation $\Delta\mu$, which requires caution when interpreting the results). The increase of PTFE particle concentration within this zone (cf. Fig. 2(a2)) may lead to the friction factor μ being controlled by the cohesive forces of both interactions (PTFE/PTFE) and (PTFE/surface). Fig. 2(c) confirms the relation between μ and the number of PTFE inside contact (denoted N_p) for the sets of parameters considered.

The figure 3 proposes a synthesis of the different tribological behavior tendencies for two granulometries. Results obtained with the previous set of parameters, are shown in Fig. 3(a) while Fig. 3(b) and 3(c) propose different “volume” parameter combinations for weak relative influence of the (oil/PTFE) interaction with respect to the (PTFE/PTFE) interaction. They show the particularity to allow for particle agglomerate formation, modifying the initial grease structure.

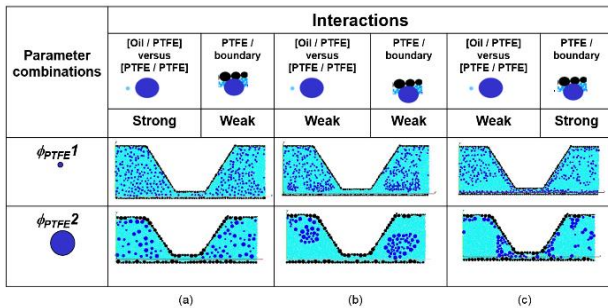


Figure 3. Different tribological behavior tendencies. (a) Homogeneous behavior; (b) Structural change, (c) Structural changes and solid third body lubrication.

In Fig. 3(b), for a second set of parameters, the initial PTFE particle distribution is modified presenting different kind of agglomerates. Their size and number depend on the granulometry. The velocity accommodation seems to generate several PTFE particle streams leading to the activation of physico-chemical interactions. Under these circumstances, no PTFE particles were entrained within the contact. In Fig. 3(c), the same “volume” combination is tested for the strongest PTFE particle- surface adhesion conditions. A “solid-like” layer with a high PTFE particle concentration is generated as example presenting on Fig. 2(b). Under such conditions, the number of PTFE particles within the confined zone of the contact and the number of particles “stuck” on the moving surface seems to increase independently of the combination and the granulometry. In particular, for the second PTFE particle size, the particles can be seen to accumulate at the contact entrance, forming grease cluster-like organisation.

EXPERIMENTAL ANALYSIS OF THE GREASE COMPONENT

Grease selection

The previous numerical analysis has focused on the relation between the macroscopic behaviour of the grease and local interaction forces for different PTFE granulometry. In order to confirm (or infirm) such tendencies, three greases and one oil were selected.

- The B-type greases, with average PTFE particle diameter of $0.1\mu\text{m}$ and 25% PTFE in volume, formulated with the PF oil (“PF-B”) or the SH oil (“SH-B”);
- The historical A-type grease, with an average PTFE particle diameter of $10\mu\text{m}$ and 10% PTFE in volume and formulated with the PF oil (“PF-A”);
- The PF oil alone.

The first couple of greases will allow to test the influence of oil and oil/PTFE interaction, while the third grease is tested to check the influence of granulometry. The oil is used to test the influence of the thickener. The different properties are summarized in Table 2.

Lubricant name	Base oil	Granulometry / Grease structure		%V of PTFE in oil	Global rheology: dynamic viscosity at 100/s - 40° (Pa.s)
		ϕ_{PTFE} (μm) in PTFE powder	Agglomerate sizes (μm)		
Grease «PF-B»	PF	0,1	Up to 50	25	6,5
Grease «PF-A»	PF	10	20-30	10	7,2 (measured by the MAP company)
Grease «SH-B»	SH	0,1	Not observed	25	4,7

Table 2. Structural and rheological properties of the three greases tested

Adhesion characterisation

As known in literature and as confirmed by DEM modelling, adhesion is a concept difficult to define and to quantitatively assess. The choice made here was to investigate this parameter for the selected greases with respect to surface samples close to real bearing ones. This is a preliminary step, still going on. During preliminary experimental work performed on an alternative tribometer [9], grease was spread on the steel sample surface through one pass with a dedicated tool that allows to control the deposited grease thickness. Microscopic observations of the greased sample surfaces were observed for investigation on real grease structure and on grease/sample adhesion conditions. Test performed for grease “PF-B”, is shown in Fig.4 and this for grease “PF-A” in Fig. 5. For the grease PF-B, the presence of significant transparent lumps (“felt” by the operator during spreading) of size up to $50\mu\text{m}$ can be observed (cf. Fig. 4 (a) or 4(b) and schematized in Fig. 4(c)). SEM pictures (Fig. 4(b)) show the presence of small rounded substructures, which are probably elementary particle agglomerates. Except the presence of these agglomerates, a good adhesion between the grease and the sample surface could be observed as the grease covers the full surface. It can be imagined that the grease sticks to the

ball, which could lead to an important entrainment grease volume beneath the ball and a possible recirculation of grease through adhesion to rotating balls, as schematized in Fig. 6(a).

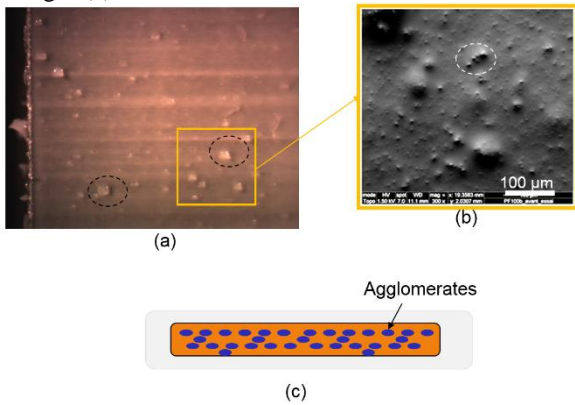


Figure 4. Grease PF-B: (a) image of the greased test sample, (b) SEM image of the surface, (c) schematics of the greased test sample morphology.

The same procedure was applied for grease “PF-A”. The lumps are also existent, with an approximate size of 20μm (cf. Fig. 5(a) and (b)) and schematized in Fig. 5(c).

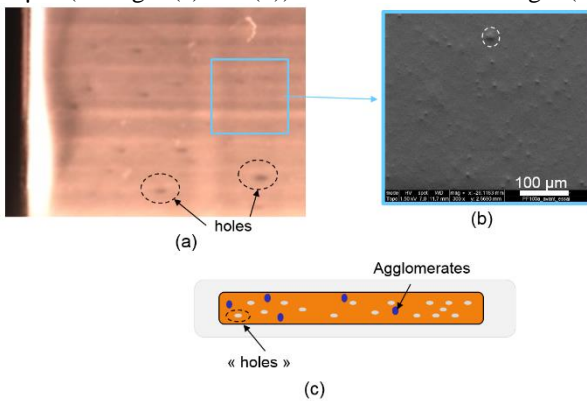


Figure 5. Grease PF-A: (a) image of the greased test sample, (b) SEM image of the surface, (c) schematics of the greased test sample morphology

The main difference with grease “PF-B” (as also “felt” by the operator during spreading) is the presence of “holes” on the sample surface. This suggests less adhesion between grease “PF-A” and sample surface, even if other volume interpretation could also be suggested (as more “elastic” volume properties). It can be imagined that there is sliding between ball and grease. This would lead to a low grease entrainment below the ball, the grease being accumulated in front of the balls or evacuated at the sides, as schematized in Fig. 6(b).

B-type grease lubricated bearing analysis

After a focus on adhesion properties, the use of grease on bearing like conditions is performed. Especially, the case presenting an unexpected behaviour when lubricated with B-type grease is selected: it is a pre-loaded double-

raw deep and angular contact bearing.

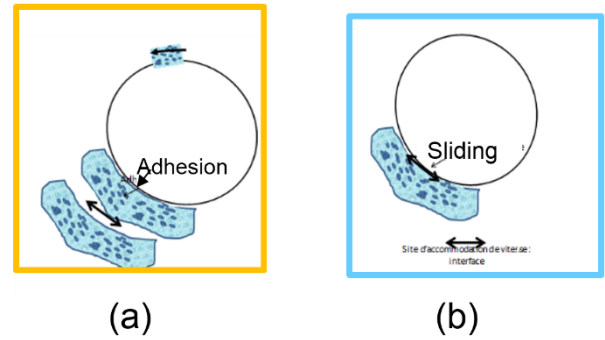


Figure 6. Schematics of the contact adhesion conditions (a) grease PF-B, (b) grease PF-A.

Preliminary operator-hand experimentations were performed on such a bearing. At low speeds, the increase of torque peaks could be “felt” by the operator when an oscillatory motion (a rotation of a few degrees around a given angular position) is applied to the bearing. Then, when a continuous motion follows the oscillatory one, a decrease of torque peaks located periodically was obtained. At high speed, torque peaks were not observed, showing reversible phenomena (as peaks disappear) in addition to transient and periodic. Based on such a preliminary work, a bearing test bench has been developed to optimize the experimental protocol in order to be able to reproduce the suspected torque peaks. The bearing test bench is presented in Fig. 7.

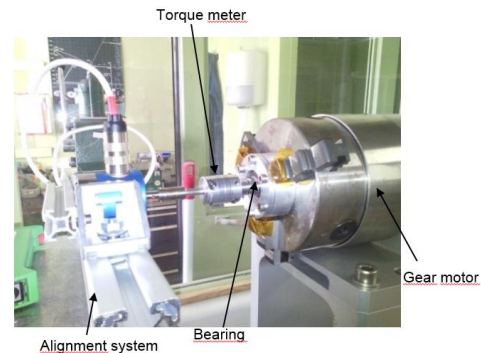


Figure 7. Bearing test bench.

The bearing external ring is tightened within a gear motor. The bearing axis is coupled with a torque meter through flexible couplings and connected to an acquisition electronic card. Automated commands impose continuous and /or oscillatory movements and allow the visualization and the measure of resulting bearing torque evolution.

Among the different tested ones, the following optimized protocol allows the discrimination of the different lubricants and is based on three steps.

In a first phase, a high velocity rotation speed is given manually to the bearing ($V > 100 \text{rpm}$) in order to erase the residual torque peaks. The average torque decreases to reach a constant value. This suggests a classical lubrication behavior with a velocity accommodation

within the grease [5] and a friction factor controlled by the grease viscosity. Then a second phase is operated in view to create torque peaks for the B-type grease (cf. Fig. 8).

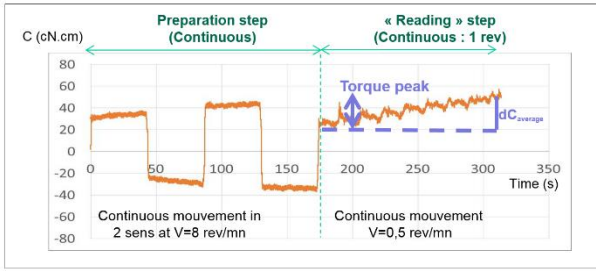


Figure 8: Bearing torque measure versus time for the grease “b” for the presented protocol

Five revolutions are applied to the bearing at 5rpm twice in both directions. During this preparation phase, the average torque increases and then becomes stable. During the third phase, one revolution is realized at 0.5rpm to measure the torque peak amplitudes: they are periodic while the average torque increases for B-type grease. To complete torque observations, some interpretations are suggested in Fig. 9.

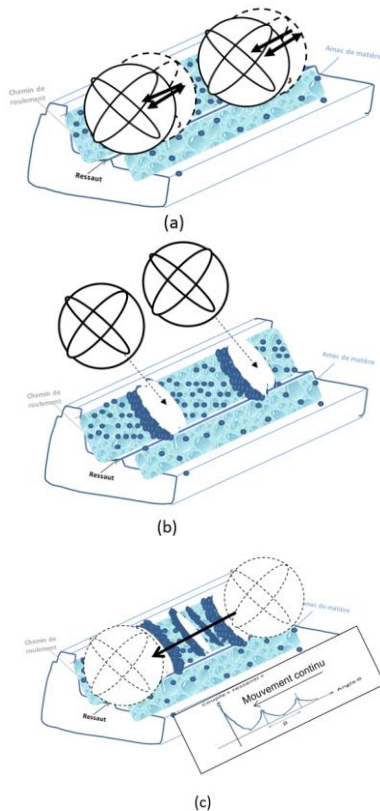


Figure 9: Reconstitution attempt for the grease PF-B in the case of the considered protocol: (a) torque peak erasure, (b) “preparation” step, (c) “reading” step.

To recall the process, first the residual torque peaks are erased (cf. Fig. 9(a)). On Fig. 9(b) periodic grease

clusters perpendicular to the rolling direction can be observed after a run. The grease is accumulated step by step in front of each ball forming clusters as observed on the internal ring surface morphologies via photonic microscopy (cf. Fig. 10). The clusters were obtained after bearing oscillatory movements that exacerbate what is obtained during the considered protocol. Between two successive clusters, no significant grease layer can be visualized, suggesting the creation of different surface areas with different physico-chemical and mechanics properties and thus friction factor change. Under these conditions, there is a possibility for the balls to have specific kinematics (rolling and/or sliding sequences), which could be causes and consequences of these grease clusters. The torque remains constant, which could mean that an equilibrium is being achieved, with grease depth and velocity accommodation location constant.

Finally, during the last phase, the velocity decrease may favour the adhesion between the grease and the balls. In the previous subsection, it was suggested that the B-type grease was sticky to the sample surface (cf. Fig. 6(a)). It can be imagined that the balls can cross over at least partly the closest clusters. The first torque peak, which is the highest measured can be associated to the first crossing over. The passage on different surface layers (with friction factor changes) can also contribute to it. If grease is entrained below the ball, a grease shearing work in volume can be expected, which could lead to grease structural changes.

For the considered B-type grease, these results firstly confirm that bearing test bench allows the reproduction of the transient, periodic but also reversible phenomena identified in preliminary operator-hand experimentations. Torque peaks could also be measured and associated to the presence of periodic grease clusters all around the periphery of the bearing rings. An average torque increase could also be identified. Noted that, if the phenomenology is reproduced, the quantitative results depend on the given solicitations.

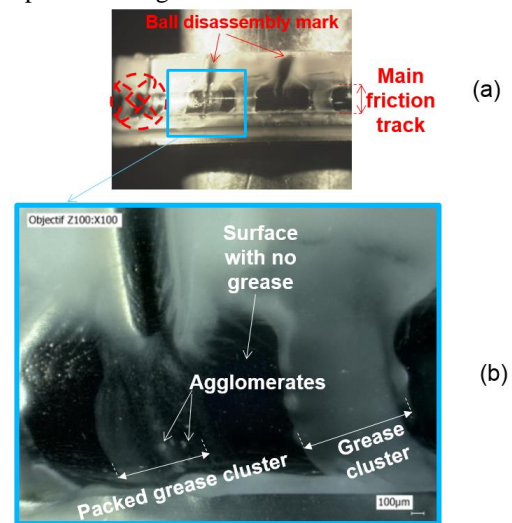


Figure 10: (a) Bearing ring surface image (photonic microscopy), (b) Zoom of (b).

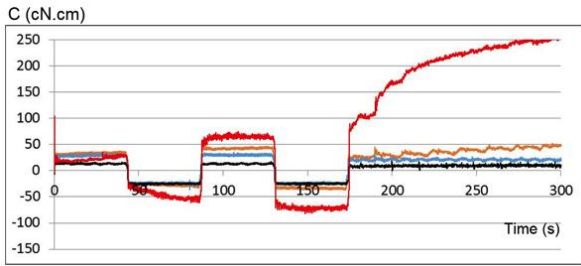


Figure 11: Torque measure versus time for the 4 selected lubricants (grease “PF-B” in orange, grease “PF-B” in blue, grease “SH-B” in red, oil PF in black) for the selected protocol

Discrimination between the selected greases: torque evolution and surface morphologies

To complete the experimental part, the interpretations performed for B-type grease are attempted to be generalized to the other selected lubricants. A reconstitution of the activated grease flows, velocity accommodation sites, and local rheology are proposed. The Fig. 11 presents the comparison of the different torques measured on the bearing test bench, with respect of the previous protocol and for the different selected greases. These experiments allow clearly the discrimination of the lubricants. Contrary to the B-type grease, PF oil and PF-A grease do not present any torque peak and the average torque remains constant. The grease SH-B presents the same behavior as the grease PF-B but is quantitatively exacerbated, with high peak torques and thus a large increase of the average torque. As the same PTFE powder was used for both B-type greases, the interactions between base oil and PTFE seems to be predominant. An attempt in the reconstitution of the dynamical scenario is presented in Fig. 12 and Fig. 13.

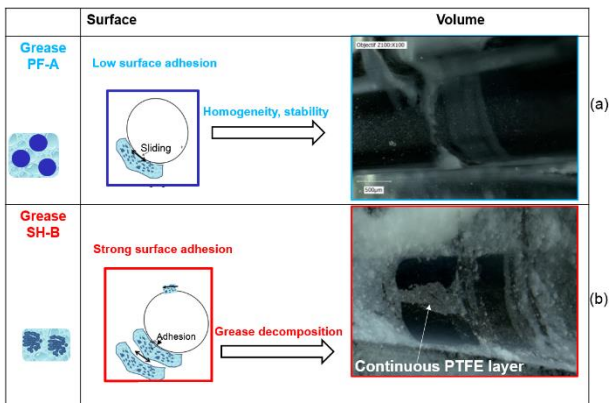


Figure 12: Reconstitution attempts for the extreme tribological behavior (a) grease “PF-A”, (b) grease “SH-B”

Grease	Schematics of the grease flows	Location of velocity accommodation	Rheology / friction μ
Oil PF		Oil volume	$\mu = \mu_{oil_viscosity}$
Grease « PF-A »		Ball/grease interface	$\mu = \mu_{interface_ball_grease}$
Grease « SH-B »		PTFE layer volume	$\mu = \mu_{solid_PTFE_3rd\ body}$

Figure 13: Reconstitution attempts for the extreme tribological behavior of the activated flows (a) oil PF, (b) grease “PF-A”, (c) grease “SH-B”

For PF oil (Fig. 13(a)), there is no accumulation of oil in front of each ball. It suggests that adhesion to surfaces is sufficient and that all surfaces are covered by oil. The accommodation is located within the oil volume. For the “PF-A” grease (Fig 12(a) and Fig. 13(b)), a low adhesion to steel surfaces was suggested, which could lead to sliding between ball and grease. In that case, a low grease entrainment below the ball can be imagined, the grease being accumulated in front of the balls or evacuated at the sides. The surfaces observed outside clusters are “clean” (very thin grease layer) and the grease seems to remain homogeneous (cf. Fig. 12(a)). The velocity accommodation is located at the interface ball/grease without the influence of the PTFE agglomerate interactions, which could explain the low torque measured. If some point have been enlightened, a question still remains on the observed homogeneity of the grease: is it a consequence of the unsheared volume (and thus its properties does not evolve) or a better stability of A-type grease (10 μ m particles) than B-type one (0.1 μ m particles). For the grease “SH-B” (cf. Fig. 12(b) and 13(c)), a strong adhesion is expected between grease and surfaces, which leads to the entrainment of an important volume of grease beneath the ball and a possible recirculation through adhesion to rotating balls. In this specific case, a PTFE/oil segregation seems to happen in the grease with the presence of a continuous layer stuck on the roller path that appears white and that is composed of solid like agglomerates of rounded particles (as in PTFE powder) suggesting a local strong PTFE ratio and oil departure from load-carrying areas. The velocity accommodation could take place within this “solidified”, “dried” layer of PTFE, which could explain the strong torque. From this last point, it remains to check if local observation can be generalized and transposable to the bearing scale.

Noted that, these results depend on kinematics because, under another protocol (as oscillatory type movement), A-type grease can present bearing torque peaks (work performed but not presented here).

CORRELATION ATTEMPTS BETWEEN MODELLING AND EXPERIMENTS

To conclude the present work, the tribological behaviors measured and identified for the selected lubricants are compared to the ones obtained by the GDEM model.

PTFE powder manufacturers parameters and model internal grease properties

The PTFE powders commercially available are usually characterized via the following parameters:

- Granulometry distribution data (average particle size, maximal size and size distribution) are given;
- Particle shape (spheres, platelets, etc..) which depends on the manufacturing process, and that are sometimes specified. They can be directly observed with microscopy.
- Specific surface measurement, related to surface energy and surface topography.

For the PTFE case, spherical elementary particles could be clearly identified and directly modelled (cf. Fig 1(a)). However, the formation of PTFE agglomerate suggests that the significant elementary element may be an agglomerate and not as single particle. Regarding the ten physico-chemical interaction parameters used in the model, they cannot be linked directly to the specific surface (related to surface energy). Combined PTFE surface energy and chemical affinities with oil may be related to the cohesion between grease components. In the model, this cohesion is mechanically represented via two parameters: a cohesive attractive force (γ) and a distance interaction (d_w) and three volume interaction are concerned (cf. Table 1): oil/oil, oil/PTFE and PTFE/PTFE. It will be necessary to go further in grease tribological behaviour understanding to find relations between numerical and physical parameters.

Surface morphologies and grease structural changes

GDEM parametric study allowed the investigation of the coupled influence of granulometry and physico-chemical grease component of interactions but also of the tribological role of PTFE. Even if the selected greases cannot be fully characterized by the input parameters of the model, the GDEM parametric study was performed for a wide range of parameters. From the different results, several comparison could be performed.

First, some homogeneous tribological behaviors could be identified; for strong relative influence of the (oil/PTFE) interaction with respect to the (PTFE/PTFE) interaction and for weak (PTFE/boundary) adhesion. Regarding the interpretations of the experimental section, the grease PF-A could be associated to this kind of behaviour. The formed agglomerates are composed of a few PTFE particles and adhesion to boundary seems to be low. Moreover, the surface morphology shows a homogeneous layer of grease. This correlation is

schematized in Fig. 14(a1) and (a2).

Then, grease structural changes could be identified for weak relative influence of the (oil/PTFE) interaction with respect to the (PTFE/PTFE) interaction and for intermediate (cf. Fig. 14(b)) and strong (PTFE/boundary) adhesion (cf. Fig. 14(c)).

In the case of strong PTFE/boundary adhesion, a solid like interface can be formed, as it could be observed for grease SH-B.

Friction and torques

The previous morphological and structural grease correlations are in reasonable agreement with the resulting friction results. The DEM model shows the clear increase of friction with the number of particle of PTFE within the contact, which is exacerbated for the SH-B which presents the highest peaks, recalled in Fig. 15.

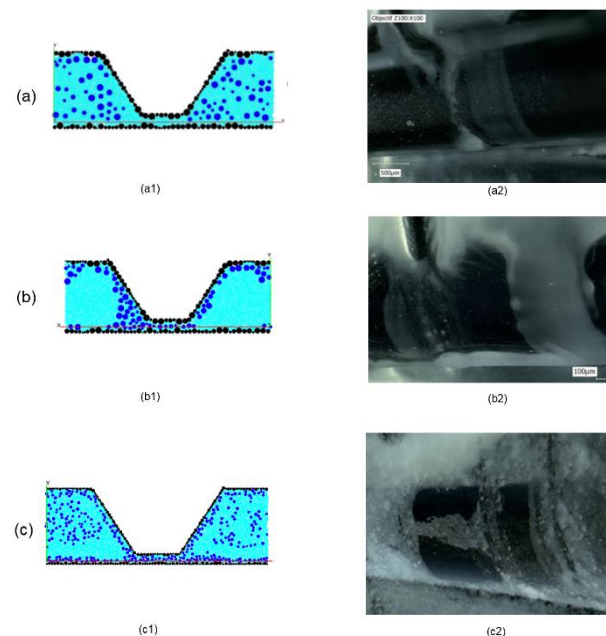


Figure 14. Correlation attempts between the DEM model and the bearing ring surface morphology. (a) Homogeneous behaviour. Case of grease PF-A (b) Grease structural changes and accumulation of agglomerated PTFE particles at the contact entrance with intermediate PTFE/boundary adhesion. Case of B-type grease. (c) Grease structural changes for strong PTFE/surface adhesion. Case of the grease SH-B.

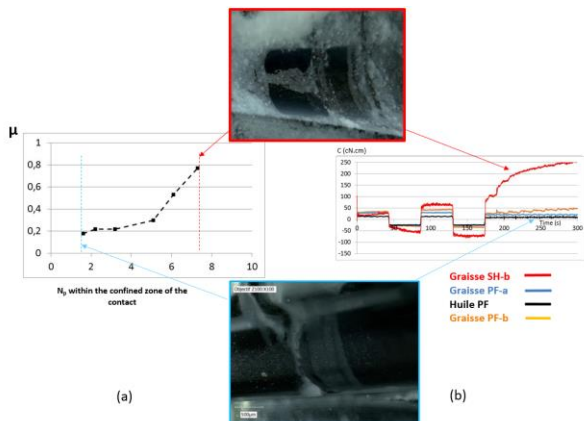


Figure 15. a) Evolution of the friction factor μ versus the %PTFE within the confined zone of the contact, (b) Evolution of the torque versus time for the selected lubricant.

CONCLUDING REMARKS AND PERSPECTIVES

In the present work, an unexpected behavior of space bearings when lubricated at low speed with a substitute PTFE “B-type” grease was investigated through a coupled numerical and experimental analysis. The use of a Grease Discrete Element Model allowed to investigate the complex discontinuous tribological behavior of such a biphasic grease and confirmed that it is controlled by the coupled influence of both grease granulometry (thickener particle sizes) and physico-chemical parameters (interaction law between particles).

In parallel, and according to numerical tendencies, the influence of the grease internal parameters was investigated experimentally on a bearing test bench by using two sizes of PTFE particles and two base oils. The considered grease behaviours were discriminated for a given protocol in terms of bearing torque evolution, of surface morphologies and grease structural changes. The measured torque peaks associated to the undesirable behaviour with B-type grease were reproduced on test bench and could be associated to both (1) the crossing over of periodic grease clusters that are perpendicular to the rolling direction by the bearing balls but also to (2) the succession of heterogeneous layers covering the ring surfaces. The considered historic A-type grease behaves as the oil alone does; i.e. without torque peak formation and without average torque increases for the considered protocol. Moreover, it remains homogeneous and presents a low boundary adhesion. The “SH-B” tribological behavior was an exacerbation of the behavior of the “PF-B”, showing here the preponderance of the oil/PTFE interaction under the selected protocol but also the structural changes of the grease with oil/PTFE segregation.

At this stage, the prediction of the tribological behavior of a PTFE grease cannot be deduced from PTFE powder granulometry and rheological data (viscosity). A

perspective would be to develop new greases by selecting proper PTFE powders among the hundreds that are commercialized but there is still work to perform to understand the PTFE/oil and PTFE/PTFE interactions when immersed in oil as a function of the powder manufacturing process, of the ratio in the mixture and of the method to mix to produce grease. The measure of adhesion grease components to boundaries is a necessary step also.

REFERENCES

- Zaretsky, E.V. (1990). Liquid lubrication in space. *Tribology International* 23(2), 1990, 75-92.
- McMurtrey, E.L. (1985). Lubrication handbook for the space industry. Part A: Solid lubricants. Part B: Liquid lubricants. *NASA/TM*, 86556.
- Buttery M. (2010). An evaluation of liquid, solid and grease lubricants for space mechanisms using a spiral orbit tribometer. *Proceedings of the 40th Aerospace Mechanisms Symposium*, NASA Kennedy Space Center, May 12-14, 2010.
- Sicre J., Vergne P., Guillaumon O., Jugniot P. (2009). Perpetuation of MAPLUB grease range, *Proc. of 13th European Space Mechanisms and Tribology Symposium, ESMATS 2009*, Vienna, Austria, 23-25 Sept. 2009.
- Berthier Y., Vincent L., Godet M. (1988). Velocity accommodation in fretting. *Wear* 125(1-2), 25-38.
- Stevens K.T. The torque behavior of grease-lubricated angular contact bearings operating at low speeds. *ESA(ESTL)46*.
- Marchetti M, Jones WR, Sicre J. (2002). Relative lifetimes of MAPLUB greases for space applications. *NASA/TM*;211875.
- Busquet M., Renouf M., Berthier Y., Sicre J. (2017). Space grease lubrication modeling: A discrete element approach. *Tribology International* 111, 159-166.
- Sicre J., Vergne P., Reynaud P., Berthier Y., Godet M. (1993). Tribological Characterization of spatial wet lubricants under vacuum. *Proceedings of the fifth European Space Mechanism and Tribology Symposium, ESA SP-334, ESTEC, Noordwijk, The Netherlands, 28-30 October 1992*, 157:163.

ACKNOWLEDGMENTS

The authors would like to thank Claude Godeau, Sylvie Descartes from LaMCoS and Guillaume Sierra, Philippe Jugniot, Olivier Guillaumon from the MAP company for their help. The authors would like to thank also the R&T of the CNES for funding this work.